Ordering of Spontaneously Formed Buckles on Planar Surfaces

Wilhelm T. S. Huck,† Ned Bowden,† Patrick Onck,‡ Thomas Pardoen,‡ John W. Hutchinson,‡ and George M. Whitesides*,†

Department of Chemistry and Chemical Biology, Harvard University, 12 Oxford Street, Cambridge, Massachusetts 02138, and Division of Engineering and Applied Sciences, Harvard University, Pierce Hall, Cambridge, Massachusetts 02138

Received October 1, 1999. In Final Form: December 31, 1999

This paper describes the spontaneous formation of patterns of aligned buckles in a thin film of gold deposited on the surface of an elastomer [poly(dimethylsiloxane), PDMS]. The surface of the elastomer is patterned photochemically into areas differing in stiffness and coefficient of thermal expansion. The gold is deposited while the surface of the patterned elastomer is warm ($T \sim 100$ °C). On cooling, shrinkage in the elastomer places the gold film under compressive stress. The buckles relieve this compressive stress. The distribution of stresses and buckle patterns is described during the pre- and postbuckling regimes using solutions from calculations describing a model comprising a thin stiff plate resting on a thick elastic foundation.

Introduction

This paper describes a method to generate a semiregular pattern of buckles in a thin film of gold on the surface of poly(dimethylsiloxane) (PDMS) and a model that accurately predicts the formation of these buckles. The experimental procedure has four steps (Figure 1). (i) A planar surface of PDMS, previously soaked in a solution of benzophenone in dichloromethane, is exposed to UV irradiation (254 nm, 10−30 min) through an amplitude photomask. The exposed regions become stiffer and less elastomeric. (ii) The sample—with its surface patterned into regions differing in stiffness (Young's modulus) and coefficient of thermal expansion—is heated to approximately 100 °C and expands. (iii) A thin metal film (5 nm of Ti as an adhesion promoter and 50 nm of Au) is deposited onto the surface by e-beam evaporation. (iv) The sample is cooled; this cooling places the gold film under compressive stress. To relieve these stresses, the thin metal film buckles.[1,2] The photostiffened regions provide more resistance to buckling than those not stiffened; this difference in response creates a pattern of buckles. This pattern of buckles is thus related to the pattern of the mask used in the UV irradiation step.

We have previously described analogous phenomena on PDMS in which the surface is patterned into bas-relief structures (Figure 2a).[3] In that work, we outlined a theory that rationalized the formation of buckles in terms of relief of compressive stress. The coefficient of thermal expansion of PDMS is 20 times larger in magnitude than that of gold. When the expanded PDMS—supporting the gold film—contracts, the gold is placed under compressive stress. In regions close to the steps in the bas-relief pattern, the stress is relieved along one direction (perpendicular to the step). The stress in the other direction is relieved by buckling of the film out of the plane; this anisotropic relief of stress produces highly regular patterns. In the

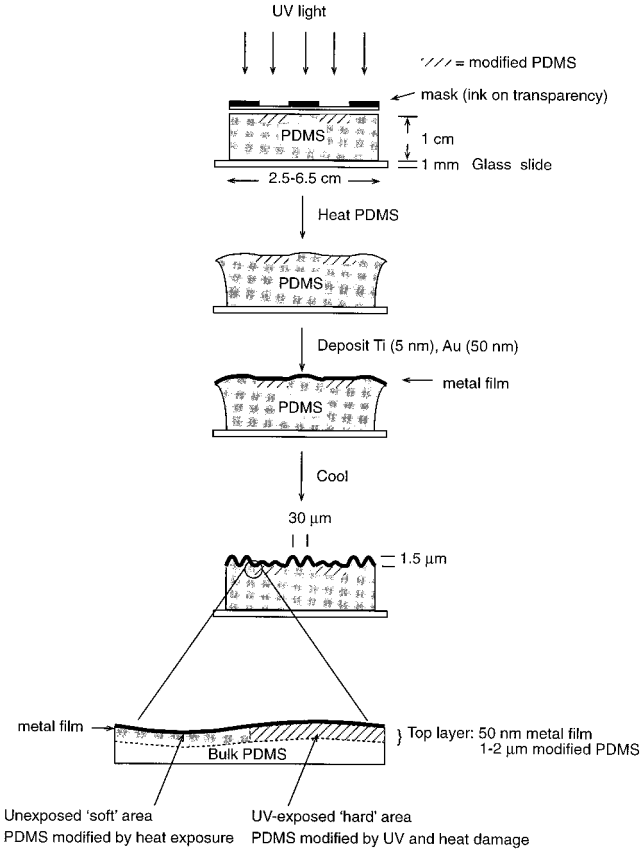

Figure 1. Outline of the procedure used to obtain aligned buckles on patterned PDMS. The surface of a block of PDMS/benzophenone was patterned via exposure to UV light through an amplitude photomask. The PDMS was placed into the e-beam evaporator. The metals were heated which caused the heating of the PDMS (the degree of expansion shown here is exaggerated). A thin film of metal is evaporated on the PDMS. After cooling to room temperature, stresses develop in the metal film, resulting in the formation of buckles. The enlarged drawing is a schematic representation of the 1−2 μm thick modified top layer on a compliant substrate of bulk PDMS.

† Department of Chemistry and Chemical Biology.

‡ Division of Engineering and Applied Sciences.

(1) Moldovan, D.; Golubovic, L. *Phys. Rev. Lett.* **1999**, *82*, 2884. Gilabert, A.; Sibillot, P.; Sornette, D.; Vanneste, C.; Maugis, D.; Muttin, F. *Eur. J. Mech. A* **1992**, *11*, 65.

(2) Crosby, K. M.; Bradley, R. M. *Phys. Rev. E* **1999**, *59*, R2542. Kinbara, A.; Baba, S. *J. Vac. Sci. Technol. A* **1991**, *9*, 2494.

(3) Bowden, N.; Brittain, Evans, A. G.; Hutchinson, J. W.; Whitesides, G. M. *Nature* **1998**, *393*, 146.

10.1021/la991302l CCC: $19.00
Published on Web 02/25/2000

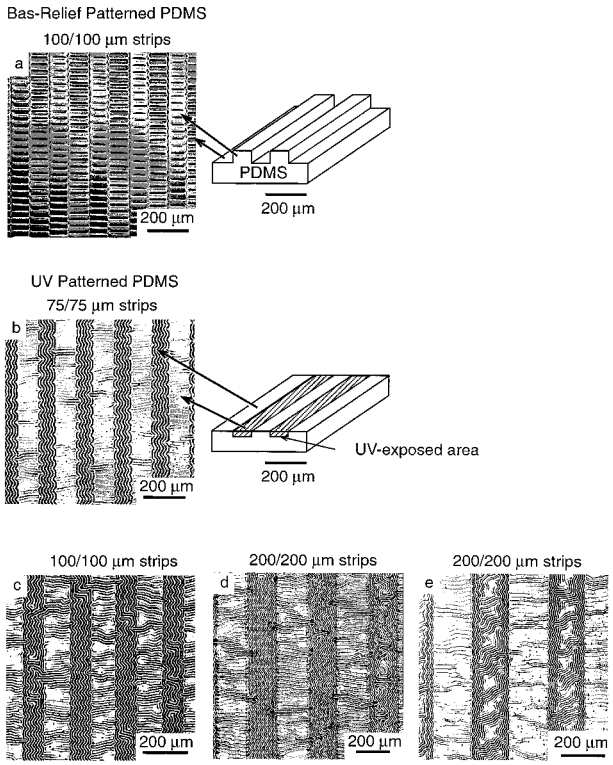

Figure 2. Alignment of buckles in thin metal film on PDMS patterned into a) bas-relief features and (b−e) regions differing in Young's modulus and coefficient of thermal expansion. There is some difference between the extent of ordering in ostensibly indistinguishably patterned regions (perhaps because of a difference in dose of UV). Parts d and e illustrate this difference. We performed over 10 evaporations and examined more than 100 samples. These optical micrographs illustrate the trends that we saw in the buckle patterns.

work reported here (Figure 2b−e), the relief of stress is more complex than in samples having surfaces patterned in bas-relief. The primary influence on the buckling pattern of the top film is the photostiffening of regions exposed to UV light. The analysis of the patterns of buckles that result from the interaction of buckling in the exposed and unexposed regions is the subject of this paper.

The techniques that we have developed for fabricating wavy structures may find uses in areas such as microelectromechanical systems (MEMS), biology, and nano- and microfabrication. These waves can function as diffraction gratings, pressure sensors, substrates to control the direction of cell growth, substrates to monitor the stress a cell places on a surface, stamps for microcontact printing, or masks for photolithography. The patterns have a sinusoidal topography that complements regular, square features produced by conventional photolithography.

Results and Discussion

Effect of UV Irradiation. PDMS is almost transparent to UV light, and although irradiation gives changes in surface stiffness, these changes require prolonged irradiation and are not reproducible. To increase both the sensitivity of PDMS to irradiation and the reproducibility of the modification of the surface, PDMS was soaked for 5 h in a 0.25 M solution of benzophenone in dichloromethane. PDMS was dried for 24 h in air, in the dark, before exposure to UV light. The benzophenone—a photosensitizer—generates radicals upon irradiation; these radicals cross-link PDMS by mechanisms we have not

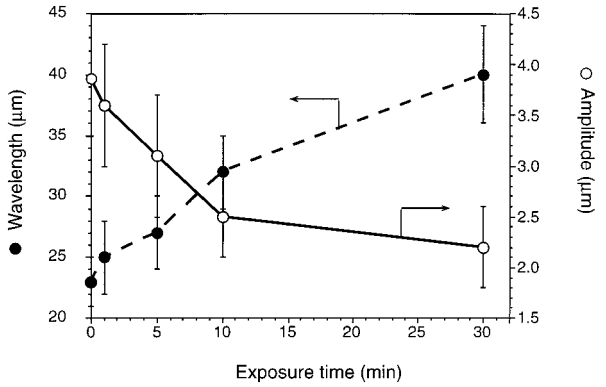

Figure 3. Dependence of the wavelength and amplitude of the buckles on PDMS to the duration of the exposure of PDMS to UV light.

established in detail.[4,5] As a result, exposure to UV light increases the Young's modulus of the top layer of PDMS. We assume in this paper a thickness of approximately 2 μm for this top layer.[3] The Young's modulus of PDMS also increases, up to a depth of 1−2 μm,[3] by heat exposure (with the probable result of additional cross-linking or curing of PDMS) during deposition of the metal film. In areas exposed to UV light, the stiffening will be largest, because the top layer will be modified by both the UV and the heat during evaporation of metal (Figure 1); in the unexposed regions, this top layer will only be modified by the heat. In this paper, we will treat the metal film (characterized by the thickness, t_m, the Young's modulus, E_m, and the Poisson ratio, ν_m) plus the modified top layer of PDMS (with parameters t_1, E_1, and ν_1 in the UV-exposed areas and t_2, E_2, and ν_2 in the unexposed areas) as one, combined bilayer plate with effective properties $\bar{t}_i$, $\bar{E}_i$, and $\bar{\nu}_i$ (with $i = 1$ or 2) on top of a thick, homogeneous, and compliant substrate of PDMS. For an equibiaxial stress state in a single infinite film, the wavelength λ of the buckles can be expressed as eq 1,[6] where the subscript s

$$\lambda \approx 4.36\bar{t}_i\left(\frac{\bar{E}_i}{(1-\bar{\nu}_i^2)}\frac{(1-\nu_s^2)}{E_s}\right)^{1/3} \qquad (1)$$

refers to the nonmodified substrate. Longer exposure times lead to an increase in the wavelength of the buckles and a decrease in the depth of the buckles (Figure 3). Although the relation between parameters of the modified PDMS and the effective thickness and Young's modulus ($\bar{t}_i$, $\bar{E}_i$) of the thin, bilayer plate is intricate (see eqs 2−6 below), eq 1 shows that an increase of Young's modulus and/or the thickness due to longer exposure times lead to an increase in the factor $\bar{t}_i\bar{E}_i^{1/3}$ and consequently to an increase of the wavelength of the buckles.

Alignment of Buckles on Patterned PDMS. Earlier experiments on surfaces patterned into bas-relief features (Figure 2a) showed buckles that aligned perpendicular to the steps. Parts b−d of Figure 2 show the alignment of buckles on alternating irradiated and nonirradiated strips on the flat surface of PDMS/benzophenone. On exposed and thus stiffer areas, the buckles align perpendicular to the boundary between the strips; on the unexposed areas, the buckles align parallel to the boundary. We can explain

(4) Egitto, F. D.; Matienzo, L. J.; Spalik, J.; Fuerniss, S. J. *Mater. Res. Soc. Symp. Proc.* **1995**, *385*, 245.
(5) Leite, C. A.; Soares, R. F.; Goncalves, M. D.; Galembeck, F. *Polymer* **1994**, *35*, 3173.
(6) Allen, H. G. *Analysis and Design of Sandwich Panels*; Pergamom: New York, 1969.

the buckling pattern qualitatively by looking at the relief of stresses in the top layer. As the temperature drops, buckling starts within the unexposed strips. The higher bending stiffness of the exposed strips constrains the buckling on the unexposed strips such that the buckles in the unexposed regions align parallel to the boundaries between strips. As the temperature is lowered further, the buckles permit the exposed strips to expand into the unexposed regions, relieving the compressive stress in the exposed strips in the direction perpendicular to the boundaries. When the exposed strips buckle, the buckles form perpendicularly to the direction of maximum compressive stress (i.e., perpendicular to the boundaries). The sinusoidal-like buckling patterns in the unexposed strips seen in Figure 2b−d develop after the exposed strips buckle, as discussed below. The examples shown in Figure 2b−d are taken from samples that displayed reasonably ordered buckling patterns; patterns such as those shown in Figure 2e were also observed.[7] Apparently, the balance of forces in the x and y directions is delicate and easily disturbed.

Modeling of Buckles on Patterned Surfaces. We developed a model to predict and explain the formation of the buckles. We will briefly sketch this model and give a more thorough description in the following paragraphs. The surface was modeled to be a thin plate that rested on a series of springs—the springs modeled the complaint, nonmodified, bulk PDMS. The physical properties of the plate were derived to represent the behavior of a two-layer system made of the gold film and the top modified PDMS layer; we will outline the important equations and leave the full derivation to another paper. The equations were used in the calibration of this model using a finite element method. We made estimates for the properties (Young's modulus, Poisson ratio, thickness, and coefficient of thermal expansion) of the modified surface; we could not measure these properties. The model was calibrated—and the parameters describing the surface layers were modified—with the measurements for the wavelengths and depths of the buckles at the various UV exposure times (Figure 3). Once this model was complete, we could explain the mechanism for the formation of the ordered waves and predict the pattern of waves on PDMS with various surface patterns. The model predicted the general characteristics of the aligned waves, but the parameters needed minor adjustments to model various patterns. We believe that these adjustments were due to variations in the properties of the surfaces from sample to sample.

The stress distribution in the thin stiff film deposited on an elastomeric polymer is modeled as a thin bilayer plate on a thick elastic foundation (see Figure 1). The differences of thermal expansion coefficients with respect to the substrate are denoted as $\Delta\alpha_m = \alpha_m - \alpha_s$ and $\Delta\alpha_i = \alpha_i - \alpha_s$, where α_s, α_m, and α_i are the thermal expansion coefficients of PDMS, the gold film, and the modified layers, respectively. Neglecting the differences in Poisson ratios ($\nu_1 = \nu_2 = \nu_m = \bar{\nu}_i \equiv \nu$), the effective properties of the bilayer plate are given by eqs 2−6.[8] Here $i = 1$ or 2, for the exposed and unexposed regions, respectively, $\bar{S}_i$ is the effective plane strain stiffness, $\bar{B}_i$ is the effective bending stiffness, $t_{Ri} = t_i/t_m$, and $E_{Ri} = E_i/E_m$.

To model the constraint imposed by the substrate on the film adequately during the prebuckling and post-buckling regimes, the substrate is modeled as an elastic foundation of continuously distributed tangential and normal springs.[9,10] The tangential stiffness is obtained by requiring the model to reproduce the in-plane film displacements for the case of alternating infinite strips of width L_i.[6] The calibration problem is solved using a finite element (FE) method.[11] The result of the calibration in each region leads to eq 7, where f is the function determined by the FE calculation.

$$\bar{S}_i = \frac{t_m E_m + t_i E_i}{1 - \nu^2} \tag{2}$$

$$\overline{\Delta\alpha_i} = \frac{t_m E_m \Delta\alpha_m + t_i E_i \Delta\alpha_i}{(1 - \nu^2)} \bar{S}_i \tag{3}$$

$$\bar{B}_i = \left(\frac{E_m t_m^3}{12(1 - \nu_m^2)}\right)\left[4(E_{Ri} t_{Ri}^3 + ((1 + t_{Ri})^3 - t_{Ri}^3)) - 3\frac{(E_{Ri} t_{Ri}^2 + ((1 + t_{Ri})^2 - t_{Ri}^2))^2}{(E_{Ri} t_{Ri} + 1)}\right] \tag{4}$$

$$\bar{t}_i = \sqrt{12\frac{\bar{B}_i}{\bar{S}_i}} \tag{5}$$

$$\bar{S}_i = (1 - \bar{\nu}_i^2)\bar{S}_i\sqrt{\frac{\bar{S}_i}{12\bar{B}_i}} \tag{6}$$

$$\frac{k_{tgi}\bar{S}_i}{E_s^2} = f\left(\frac{L_i E_s}{\bar{S}_i(1 - \nu_s^2)}\right) \tag{7}$$

The stiffness of the normal springs k_{ni} was calibrated using the solution of Allen[6] in such a way that the model problem reproduces the exact critical buckling stress and wavelength (λ) for an infinite uniform film:

$$k_{ni} = \left(\frac{3E_s^4}{(1 - \nu_s^2)^4}\frac{1 - \bar{\nu}_i^2}{\bar{E}_i}\right)^{1/3}\frac{1}{2\bar{t}_i} \tag{8}$$

Specification of the Parameters for the Model. The characteristics of the metal film and of the PDMS substrate are known.[12] The properties of the UV-modified PDMS layers are not known. It is possible to use the wavelengths measured experimentally to estimate the thicknesses: the wavelengths range from ∼20 μm in unexposed areas to ∼40 μm in exposed areas (Figure 3). As a first approximation, we can assume (i) that eq 1 applies in the present situation and (ii) that the UV exposure and the heat during deposition typically increase the stiffness of the PDMS only moderately: $E_1 = 2-4E_s$ and $E_2 = 1-2E_s$.[3] One can then estimate, using eqs 1−7, that $t_1 \approx 2.2$ μm and $t_2 \approx 2.7$ μm to give a wavelength of 20 μm in both areas when $E_s = 50$ MPa. The wavelength of the buckles is only weakly dependent on Young's modulus of the modified PDMS for a given thickness of the modified layer. One of the contributions of the model will be a more precise determination of these parameters (see below). Typical

(7) We studied the formation of patterns in the interior of the samples, well away from the edges of the specimen where the prebuckling stress in the gold film is highly nonuniform. In interior regions, the prebuckling stress is nearly uniform and equibiaxial.

(8) Onck, P.; Pardoen, T.; Hutchinson, J., in preparation.

(9) Timoshenko, S. P.; Gere, J. M. *Theory of Elastic Stability*; McGraw-Hill: New York, 1961.

(10) Brush, D. O.; Almroth, B. O. *Buckling of Bars, Plates and Shells*; McGraw-Hill: New York, 1975.

(11) In this FE model, the plates differed only by their thermal expansion coefficients ($\Delta\alpha_1$ and $\Delta\alpha_2$). Both plates were on top of a continuous very thick compliant substrate characterized by the elastic constants E_s and ν_s.

(12) $t_m = 50$ nm, $E_m = 82$ GPa, $\nu_m = 0.33$, $\Delta\alpha_m \approx \alpha_s \approx 10^{-4}$ °C^{-1}, $E_s \approx 20-50$ MPa (depending on the cross-linking density), and $\nu_s = 0.48$.

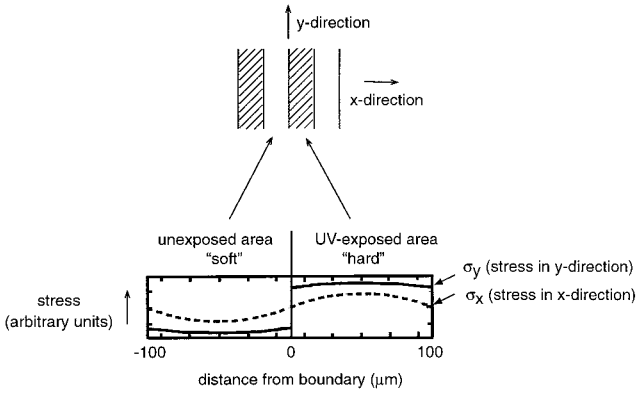

Figure 4. Schematic representation of the compressive stresses in the *x* (perpendicular to the step) and *y* (parallel to the step) directions.

values for the parameters in eq 5 indicate that $\overline{\Delta\alpha_i}$ must be always very close to $\Delta\alpha_m$. Since $\alpha_m \ll \alpha_s$, the thermal expansion mismatch is nearly uniform with $\overline{\Delta\alpha_i} \approx \Delta\alpha_m \approx -\alpha_s$.

Prebuckling Stress Analysis. Only the tangent springs and relations (2)−(4) enter the analysis of the prebuckling stress problem for the long strips. The problem is analyzed using periodic boundary conditions. For relatively narrow strips, the compressive stress distribution as a function of distance from one of the boundaries is schematically shown in Figure 4. The stresses are larger on the hard, exposed areas than on the unexposed areas. Within the less stiff areas, σ_x is larger than σ_y, and conversely. These differences are exaggerated: in reality, the prebuckling stresses are nearly uniform and equibiaxial because $\overline{\Delta\alpha_1} \cong \overline{\Delta\alpha_2}$ and $\bar{S}_1 \cong \bar{S}_2$.

Buckling Analysis. The analysis of the buckling and postbuckling of an elastic plate on an elastic foundation is a highly nonlinear problem. The general-purpose FE code ABAQUS[13] has been used to solve the boundary value problems corresponding to different patterns. Owing to the symmetry of the patterns, the analysis can be performed on unit cells with appropriate periodic boundary conditions. In the FE model the bilayer film is discretized by many shell elements whose nodes are attached to two tangent springs (at 90° to one another) and one normal spring.[14] The temperature was lowered incrementally at each step of the calculation.

Parts a−c of Figure 5 show the evolution of the out-of-plane displacement within the periodic computational cell as a function of the temperature decrease ΔT.[15] The boundary conditions in this calculation enforce symmetry along the four sides of the cell. Figure 5a (ΔT = 45 °C) shows that buckling has already started in the unexposed area. At ΔT = 50 °C, buckling develops rapidly in the UV-exposed area in the orthogonal direction (Figure 5b). Finally, at ΔT = 80 °C, the longitudinal buckles undergo significant wrinkling (Figure 5c). Wrinkling of the longitudinal buckles is also observed experimentally (Figure 2b−d). The wavelengths in the exposed and unexposed areas are equal to about 12 and 30 μm, respectively, matching the experimental values. An amplitude of the buckles of 2 μm for ΔT = 80 °C is in good agreement with the experiment. Because of the approximations of the model[16] and the uncertainty in the properties of the modified layers, some trial and error adjustment of the parameters of the model was necessary to arrive at the patterns of Figure 5. More precisely, the effective properties of the UV-exposed area do not appear to be accurately predicted by eq 1 and therefore had to be slightly tuned.

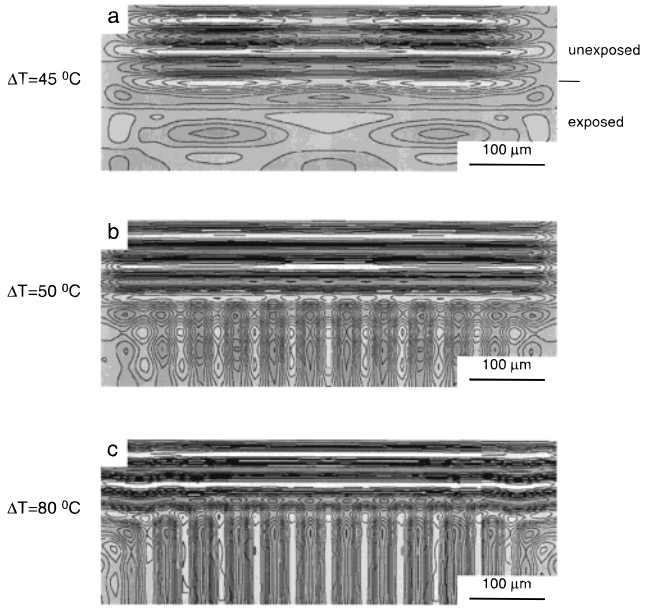

Figure 5. Simulated buckling patterns on infinitely long, parallel strips as the temperature of the system is decreased. The top half of each pattern was not exposed to UV light, and the bottom half was exposed to UV light. (a) Start of buckling on a nonexposed area (ΔT = 45 °C). The buckles are the long parallel lines parallel to the interface of the exposed and unexposed regions. (b) Start of buckling on UV-exposed area (ΔT = 50 °C). The buckles in the unexposed region are perpendicular to the interface of the exposed and unexposed regions. (c) Wrinkling of longitudinal buckles (ΔT = 80 °C). The contours show the heights of the surface.

Complex Patterns. Parts a−c of Figure 6 show the alignment of buckles around more complex patterns that have been generated photolithographically in PDMS. The alignment of buckles in Figure 6a on a substrate patterned with unexposed 200 × 200 μm squares in an exposed background illustrates the parallel and perpendicular alignment of the buckles on the two substrate regions. A similar pattern is observed in the FE model calculations, where symmetry conditions have been imposed on the region shown in Figure 6d. This example illustrates the potential of the model. The range of parameters for which the experimental pattern could be reproduced is not very large, and the parameters chosen to produce Figure 6d were slightly different from those for the strip problem.[17] We had to modify the parameters used for the long strips in order to accurately predict the square patterns. This tuning does not cast doubts on the modeling for two reasons. First, the parameters have not been tuned by

(13) *ABAQUS Version 5.7 User's Manual*; Hibbit, Karlsson, and Sorensen: Providence, RI, 1997.

(14) A tiny initial geometric imperfection was necessary to trigger the buckling. A sinusoidal imperfection typically equal to $t_i/20$ has been used. It was verified that this imperfection does not influence the solution.

(15) These results have been obtained for strips of 110 μm width using E_s = 50 MPa, t_1 = 1.4 μm, t_2 = 2.2 μm, E_1 = 160 MPa, E_2 = 60 MPa, $\nu_1 = \nu_2 = 0.3$, and $\alpha_s = 1.5 \times 10^{-4}$ °C^{-1}, resulting in the following effective properties: $\bar{E}_1$ = 6.7 GPa, $\bar{E}_2$ = 5.4 GPa, $\bar{t}_1$ = 0.64 μm, $\bar{t}_2$ = 0.78 μm, $\overline{\Delta\alpha_1} = \overline{\Delta\alpha_2} - 1.5 \times 10^{-4}$ °C^{-1}, and $\bar{\nu}_1 = \bar{\nu}_2 = 0.3$.

(16) The main approximations or assumptions of the model are (i) the bilayer plate is considered as one plate with homogeneous properties, (ii) springs adequately model the substrate, (iii) the calibration of the springs, and (iv) the use of identical Poisson ratios for the two components of the bilayer plate.

(17) It should be noted that the model is relatively sensitive to small variations in the governing parameters (characteristic lengths as well as elastic properties). The same sensitivity to UV exposure time and other processing variables is observed in the experimental patterns.

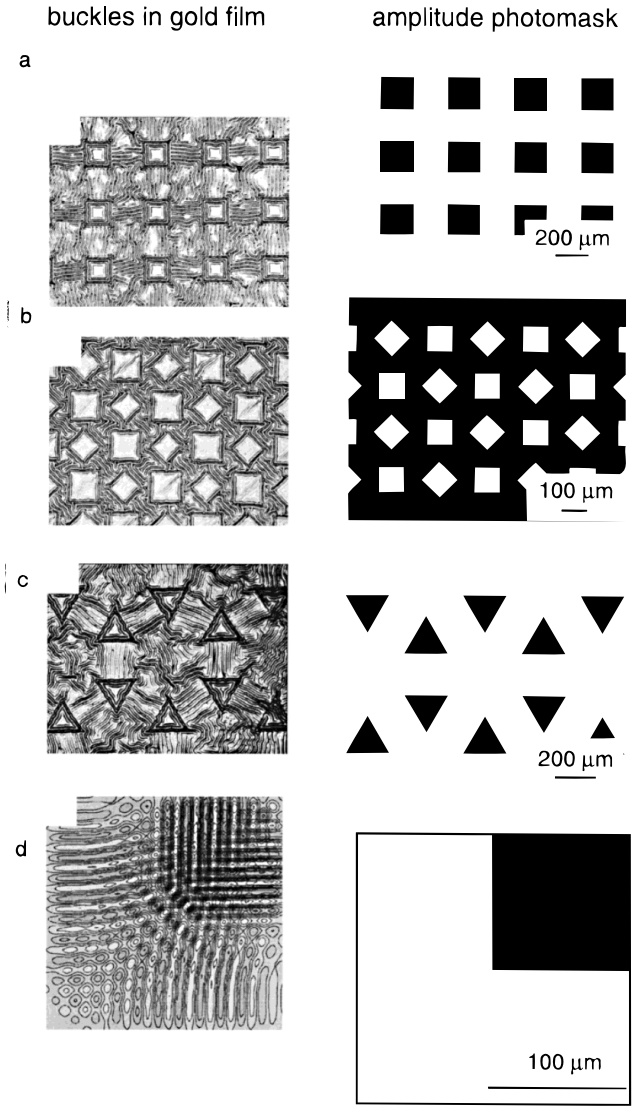

Figure 6. (a–c) Examples of more complex patterns imprinted on the surface of PDMS and the alignment of buckles around these patterns. (d) Simulated buckling pattern around the corner of a square.

more than 10%. Second, the experimental conditions were not completely reproducible from experiment to experiment so the properties of the modified layers should also vary. Without the modifications the model predicted wavelengths, amplitudes, and order of the waves that were similar to those that we observed. The parameters of the model were adjusted to exactly model the wavelengths and amplitudes for the sample; the order of the waves was not an adjustable parameter. The model correctly predicted the order of the waves before and after the small adjustments were made to the parameters describing the surface layer.

Summary of the Model. The two successes of the model are that it successfully explains how the waves formed (and why the waves were ordered) and it predicts the pattern of waves for a corner feature in the PDMS. Reasonable estimates of the properties of the surface gave good agreement between the experimental results and the model. The general application of the model is limited by our experimental methods for producing the surfaces. We believe that the UV treatment of the surfaces is not completely reproducible from sample to sample, so variations will exist in the thickness of the UV-treated layers and in the physical properties of these layers; these variations require some minor adjustments of the model from sample to sample.

Conclusions

We have developed a new procedure to form aligned patterns of buckles on planar surfaces that are patterned by a photolithography process. The buckling pattern is dependent on Young's modulus and coefficient of thermal expansion of the surface. The aligned patterns are more complex and less ordered than those obtained for the bas-relief system.[3] Simulations using a FE procedure accurately predict the buckling pattern; the success of these simulations clarifies the mechanism of the formation of the buckles. This knowledge can be used to predict buckling patterns on arbitrarily patterned substrates. We believe that these patterns of buckles will be useful in optical devices as diffraction gratings and in microfluidic devices in making channels with microstructured walls.

Acknowledgment. This research was supported by NSF (DMR 94 00396 and 98 0363) and by DARPA NSF (ECS 97 29405). W.T.S.H. gratefully acknowledges The Netherlands Technology Foundation; N.B. was supported by a predoctoral fellowship of the DOD; P.O. acknowledges a fellowship of the Royal Netherlands Academy of Arts and Sciences; T.P. was supported by the Fonds National de la Recherche Scientifique, Belgium, by the Université Catholique de Louvain, and by a fellowship of the Belgian American Educational Foundation, Inc.

LA991302L